The Egyptian Journal of Radiology and Nuclear Medicine (2016) 47, 377–385

Egyptian Society of Radiology and Nuclear Medicine

The Egyptian Journal of Radiology and Nuclear Medicine

www.elsevier.com/locate/ejrnm
www.sciencedirect.com

ORIGINAL ARTICLE

Role of MRI in the assessment of treatment response after radiofrequency and microwave ablation therapy for hepatocellular carcinoma

Bahaa Eldin Mahmoud Hussein Mahmoud [a,*], Shaima Fatooh Elkholy [a], Mohamed Mahmoud Nabeel [b], Ashraf Omar Abdelaziz [b], Tamer Elbaz [b], Hend Ibrahim Shousha [b], Mostafa Ibrahim [b], Ahmed Hashem [b], Ahmed Hamdy Ramadan [c], Ahmed Hosni Kamel Abdelmaksoud [a]

[a] *Department of Diagnostic and Interventional Radiology, Cairo University, Egypt*
[b] *Department of Tropical Medicine, Cairo University, Egypt*
[c] *Department of Internal Medicine, Cairo University, Egypt*

Received 1 March 2015; accepted 19 January 2016
Available online 5 February 2016

KEYWORDS

Dynamic MRI;
Diffusion imaging;
Radiofrequency ablation;
Microwave ablation;
Hepatocellular carcinoma

Abstract *Purpose:* The purpose of this study was to assess the role of dynamic contrast enhanced and diffusion MR imaging in the detection of tumor viability after radiofrequency and microwave ablation therapy of hepatocellular carcinoma.
Subjects and methods: The study was done on 50 patients with HCC underwent radiofrequency or microwave ablation. Patients were classified into resolved group if there's no MRI evidence of tumor viability at the ablated lesion and unresolved group if there's evidence of tumor viability.
Results: In the early 1 month post-ablation period, heterogenous signal of the ablation zone in the precontrast T1 and T2 images was noted that gradually become more homogenous in the 3–12 months follow-up. Ill defined persistent perilesional enhancement is considered as a benign finding that was present in 100% of patients imaged within the 1st month and persists only in 5% after 9–12 months. The mean ADC value of the malignant lesions was $0.91 \pm 0.09 \times 10^{-3}$ mm^2/s, while the mean ADC value of the benign post-ablation parenchymal changes was $1.29 \pm 0.12 \times 10^{-3}$ mm^2/s with a cutoff value of 1.05×10^{-3} mm^2/s.
Conclusion: MRI provides a powerful tool in the assessment of treatment response after RFA and MWA of hepatocellular carcinoma.

* Corresponding author. Tel.: +20 01004993534.
E-mail address: bahaa.mahmoud@kasralainy.edu.eg (B.E.M.H. Mahmoud).
Peer review under responsibility of The Egyptian Society of Radiology and Nuclear Medicine.

http://dx.doi.org/10.1016/j.ejrnm.2016.01.007

1. Introduction

Hepatocellular carcinoma (HCC) is one of the most common cancers worldwide, and has a poor prognosis unless treated. Generally, surgical resection is the gold standard therapy for HCC. Another treatment option is liver transplantation which is theoretically the best treatment for HCC. Currently, ablative therapies are alternative choice for patients with liver tumors who are not eligible for surgery (1). Thermal ablation is achieved by using heat (radiofrequency ablation, microwave ablation, laser ablation) or cold (cryoablation). Among all the ablative techniques, RF ablation is the one of the most widely used for both primary and secondary malignances of the liver, but all hyperthermal techniques produce coagulation necrosis, and demonstrate similar imaging features on follow-up studies (2).

Monitoring tumor response to locoregional therapy is an increasingly important task in oncologic imaging. Early favorable response generally indicates effectiveness of therapy, and may result in significant survival benefit. Early identification of treatment failure is also critical in patient management, since a repeat treatment cycle can be performed if liver function is maintained, before disease progression occurs. CT and MRI have been used to depict hepatic lesions, to guide the intervention process, and to evaluate the response of malignant liver lesions after minimally invasive local therapies. MRI has been described as superior to CT in detecting and following up ablated lesions because of its known higher sensitivity and specificity (3).

Recent advances in the development of functional imaging techniques have provided the ability to detect microscopic changes in tumor microenvironment and microstructure, thus allowing the assessment of tumor response after locoregional treatment by observing alterations in tumor viability, perfusion or vascularity. Diffusion weighted MR imaging is useful in the follow-up imaging after RF ablation. ADC-based evaluation of signal alterations adjacent to the ablation zone may contribute to the identification of local tumor progression and nontumoral post-treatment tissue changes (4,5).

2. Subjects and methods

2.1. Patients

This study included 50 HCC lesions in 50 patients underwent radiofrequency or microwave ablation over a period of 21 months (July 2012–March 2014). 35 patients underwent radiofrequency ablation and 15 patients underwent microwave ablation. The patients' ages ranged between 45 and 81 years (mean age 60); 42 patients were males and 8 patients were females. All patients had liver cirrhosis related to chronic viral hepatitis. Written consents were obtained from all patients. Exclusion criteria include tumors other than hepatocellular carcinoma and contraindications to magnetic resonance imaging, e.g. claustrophobia and cardiac pacemakers.

2.2. Post-procedural MR imaging

Patients were scheduled to undergo MRI within 1 month after ablation. If there is no evidence of residual/recurrent lesions, follow-up was arranged to be after 3 months from the first MRI and then every 6 months for the first two years after ablation. In our study 30 patients were examined 1 month after the ablation, 33 patients within 4–6 months and 20 patients within 9–12 months after ablation. The variability of time was related to clinical practice and does not affect our results.

MRI was performed using Philips 1.5 Tesla MRI scanner (Achieva). Precontrast sequences were axial T1, T2 and SPAIR, coronal T1 and T2 and Diffusion imaging. Diffusion imaging was performed before the dynamic study using respiratory triggered fat suppressed single-shot spin echo echoplanar sequence. It was obtained by applying three different b values of 0, 500, and 1000 s/mm^2. Dynamic study was then performed after manual bolus injection of 0.1 mmol/kg body weight of Gd-DTPA, flushed with 20 ml of sterile saline solution via the antecubital vein. Dynamic imaging was done using 3D GRE T1 sequence (THRIVE = T1 High Resolution Isotropic Volume Examination). A dynamic study consisted of one precontrast series followed by four successive postcontrast series including multi arterial and portal phases with 19–21 s intervals (17 s for image acquisition with breath-holding and 2–4 s for re-breathing) and this is followed by 5-min delayed phase imaging. All patients were imaged in end expiration to limit the risk of image misregistration. Acquisition parameters of the dynamic study were TR 4.4 ms, TE 2.1 ms, flip angle 10°, matrix size, 172 × 163, field of view 300–350 mm and slice thickness 2–3 mm.

2.3. Imaging analysis and interpretation

Magnetic resonance images were analyzed using the available workstation (Phillips Extended MR Workspace, 2.6.3.5 Netherlands) by two abdominal radiologists reading independently. The readers had experience of 5 and 12 years in abdominal MR imaging.

The morphological features of the ablation zone studied include size, border and signal intensity at T1 and T2 images that were classified as high, low or heterogenous. Dynamic study analysis: Arterial and portal phase dynamic subtraction was performed which is automated process available on the workstation. Subtraction color coded mapping is then performed. Pattern of enhancement in the dynamic imaging, subtracted images and color mapping was then studied.

Quantitative diffusion analysis (ADC measurement): ADC maps were generated on the workstation. ADC was calculated with linear regression analysis of the function $S = S0 \times \exp(-b \times \mathrm{ADC})$, where S is the signal intensity after application of the diffusion gradient, and $S0$ is the signal intensity at a b value of 0 s/mm^2. The three b values were used for ADC calculation. The ROI included the entire ablation zone. Another area of 2 cm diameter in the cirrhotic liver parenchyma was also measured in each case as a control. In case of focal hyperintensity within or at the margins of the ablation zone that suspects recurrence, its ADC value was calculated.

2.3.1. Dynamic study interpretation

Arterial phase enhancement: it should be confirmed by the subtraction images and color map (to prove that the high signal in the arterial phase is due to enhancement and not due to the original precontrast high T1 signal). *Contrast washout*: Decrease in the enhancement on delayed phase imaging when

compared with early phase imaging. *Presence of ill-defined perilesional parenchymal enhancement* that represents post-interventional reactive changes: this is defined as early phase enhancement beyond the ablation zone on the surrounding liver parenchyma that persists or becomes homogenous to the enhancing liver parenchyma in the delayed phase. Perfusion changes may occur in cases of injury of the portal vein or traumatic arterio-portal shunting. *Well defined enhancement at the margin of the ablation zone* represents either granulation tissue or recurrent neoplastic lesion. The granulation tissue will appear as thin rim with persistent or delayed phase enhancement, while recurrent or residual neoplastic lesion will show nodular or hallow enhancement during the arterial phase with delayed washout.

2.4. Statistical analysis

- Descriptive analysis was done and results are expressed as mean ± standard deviation or number (%).
- Comparison between mean values of ADC in the studied groups was performed using unpaired *t* test.
- *P* value less or equal to 0.05 was considered significant and less than 0.01 was considered highly significant.

2.5. The standard of reference

It was difficult to obtain pathologic confirmation in most cases because most of the patients do not undergo surgery. In addition, biopsy may result in sampling error due to technical difficulties. So, the standard of reference was as follows:

Benign findings (*resolved lesions*) *are considered if* the findings regress or disappear in the follow-up studies
Residual/recurrent HCC (*unresolved lesions*) *is considered if*:

- Increase in the size of the ablation zone when comparing the images obtained <4 months after treatment with those obtained 4–6 and >6 months after treatment.
- Focal area at the margin of the ablation zone shows early or late arterial phase enhancement that must be proved by the subtraction and color map images and contrast washout where drop of signal occurred in the delayed phase. Diffusion restriction is also considered as a sign of recurrence in the presence of positive dynamic findings.

3. Results

The signal intensity of the entire ablation zone in the non-enhanced T1 and in the T2 weighted images was studied (Fig. 1) and we found that 66.6% of the patients imaged within the 1st month after ablation show heterogenous high T1 and low T2 signal, 20% show homogenous high T1 and low T2 signal and 13.3% show homogenous low T1 and high T2 signal. While in the 4–12 months imaging most of the ablation zones elicits homogenous high T1 and low T2 signal (78.7% of patients imaged within 4–6 months and 80% of patients imaged within 9–12 months).

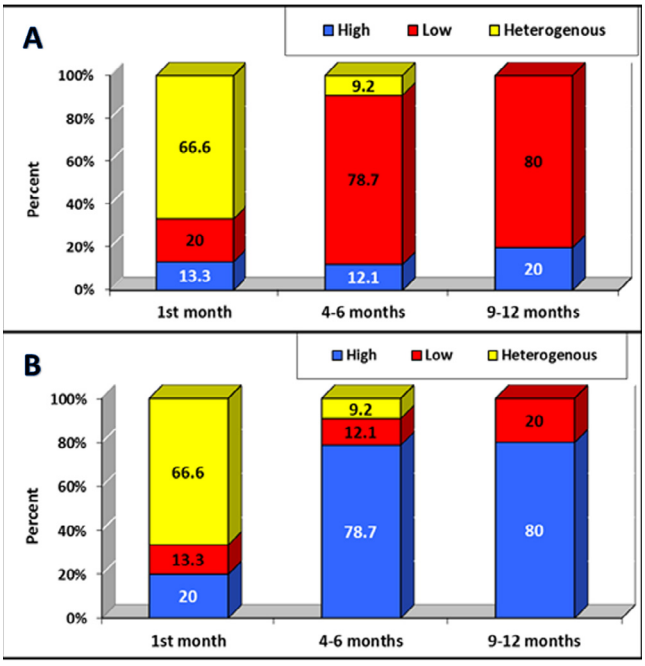

Fig. 1 (A) Signal intensity of the ablation zone in the T2 images. (B) Signal intensity of the ablation zone in the T1 weighted images.

There was no significant statistical difference in the signal intensity of the entire ablation zone between the resolved and unresolved groups or between the microwave and radiofrequency ablated lesions.

37 patients (74%) have resolved lesions while 13 patients (26%) have recurrent or residual tumor viability. The types of the tumor recurrence were studied and we followed the classification of Chopra et al. (6) and we found that nodular type was the most common and detected in 76.9% of cases followed by the halo type and the gross enlargement type those detected in 7.7% for each. More than one type of recurrence was seen in one patient (7.7%) where there were nodular and halo recurrence (Fig. 2).

We also studied the signal intensity of the recurrent lesions in the unenhanced T1, T2 and diffusion weighted images and we classified the signal intensity of the lesion into intermediate, high or low signal (relative to the ablation zone). We found 77% of the recurrent lesions elicit high T2 signal and only 31% of the lesions elicit low T1 signal. This shows that T2 weighted images is superior to non-enhanced T1 weighted images in detection of tumor recurrence.

We classified the signal intensity of the recurrent/residual lesion in the diffusion weighted images at *b* values 1000 into two types: intermediate or high signal (relative to the signal of the ablation zone). 12 out of 13 lesions elicit high signal and 1 lesion elicits intermediate signal. In the lesion with intermediate signal in the diffusion images, the dynamic study detected the lesion and this was proved by PET-CT.

We studied the presence of ill defined perilesional enhancement. It was found to be a benign finding (based on the follow-up study) that represents reactive inflammatory and vascular changes of the liver parenchyma adjacent to the ablation zone.

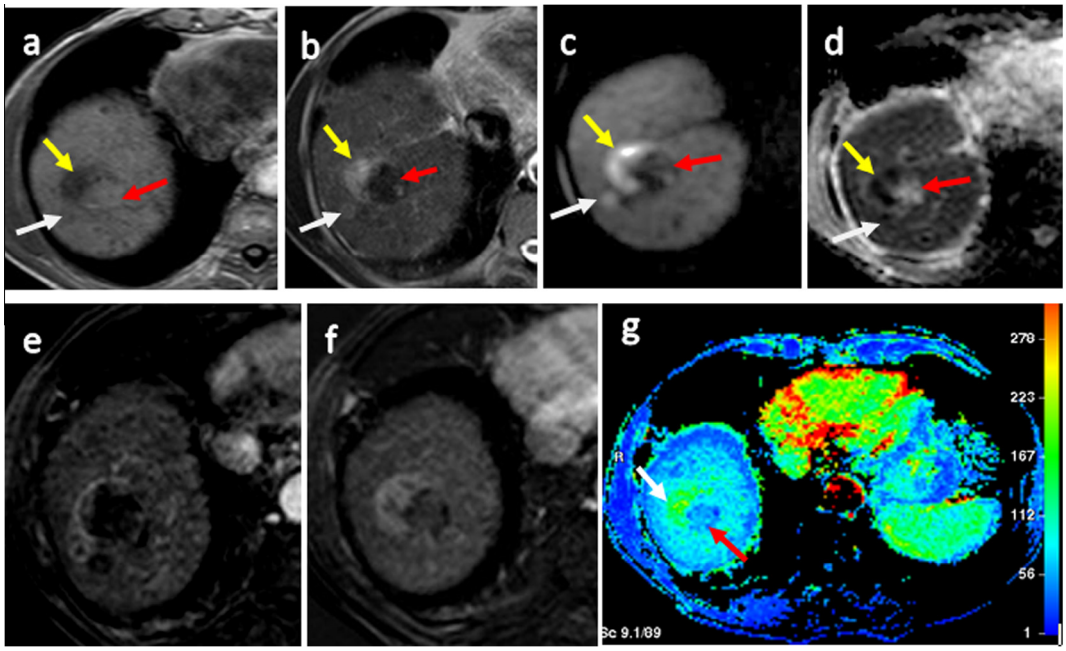

Fig. 2 58 years old male imaged 4 months after microwave ablation of right hepatic lobe hepatocellular carcinoma. (a and b) Axial T1 and T2 WIs. The ablation zone shows central area of coagulation necrosis eliciting high T1 and low T2 signal (red arrows) with a small nodule (white arrows) and thick halo (yellow arrow) at its margins. (c) Diffusion WIs and (d) ADC map at the same levels show restricted diffusion of the small nodule (nodular type of recurrence) and the thick rim (halo type of recurrence) in contrast to the center of the lesion that shows free diffusion. (e and f) Late arterial phase subtracted images. The enhancement of the nodule and halo at the margin of the ablation zone becomes more evident in the late arterial phase. Also this appears more obvious at the color map images (g) where the ablation zone (red arrows) appears non-enhancing relative to the liver while the recurrent tumor at the margin of the lesion shows intense enhancement (white arrows).

These areas exhibit mild hyperintensity in the diffusion imaging. This was present in 100% of patients imaged within the 1st month after ablation. This persists in 9% of patients imaged at 4–6 months and only in 5% after 9–12 months.

The presence of well defined thin rim of marginal enhancement was also studied. This was present in 93% of patients imaged within the 1st month after ablation, 81% in patients imaged at 4–6 months after ablation and 45% in patients imaged 9–12 months after the ablation.

The ADC values of the entire ablation zones, suspected recurrent lesions, surrounding post-ablation parenchymal changes and cirrhotic liver were calculated for the different study groups (table 1) and we found that the mean ADC value of the entire ablation zone in the RF ablated lesions (whether resolved or non-resolved) was $1.38 \pm 0.19 \times 10^{-3}$ mm^2/s while for the microwave ablated lesions it was $1.30 \pm 0.16 \times 10^{-3}$ mm^2/s. We found the mean ADC value of the recurrent or residual lesions in the malignant group (whether post-RFA or MWA) was $0.91 \pm 0.09 \times 10^{-3}$ mm^2/s while the mean ADC value of the surrounding benign post-ablation parenchymal changes was $1.29 \pm 0.12 \times 10^{-3}$ mm^2/s. The ADC value of the cirrhotic parenchyma was also measured as a control and ranged from 0.99 to 1.32×10^{-3} mm^2/s (mean 1.18 ± 0.07).

Then comparison between different study groups was done (table 2) and we found that the mean ADC value of the entire ablation zones was significantly higher than mean ADC of the cirrhotic liver parenchyma (p value 0.0001). The mean ADC value of the recurrent lesions was significantly lower than the mean ADC of the entire ablation zones (p value 0.0001). The mean ADC value of the recurrent lesions was significantly lower than the mean ADC of the cirrhotic liver parenchyma (p value 0.0001). The mean ADC value of the post-treatment benign reactive tissue changes was significantly higher than

Table 1 Mean ADC values of cirrhotic liver parenchyma, entire ablation zone, malignant lesions and reactive tissue changes.

Category	No.	Minimum ADC	Maximum ADC	Mean ADC	SD
Cirrhotic parenchyma	50	0.99	1.32	1.18	0.07
Entire ablation zone in RF ablated lesions	35	1.11	1.91	1.38	0.19
Entire ablation zone in MW ablated lesions	15	1.01	1.62	1.30	0.16
Malignant lesions	13	0.74	1.1	0.91	0.09
Reactive tissue changes	30	0.98	1.45	1.29	0.12

Table 2 Comparison between the mean ADC values of the study groups.

Entire ablation zones in all patients (n = 50)	Cirrhotic parenchyma in all patients (n = 50)	ADC ratio	P value
1.36 ± 0.18	1.18 ± 0.07	1.15	0.0001**
Residual malignant or recurrent lesions (n = 13)	Entire ablation zones in all patients (n = 50)	ADC ratio	P value
0.91 ± 0.09	1.36 ± 0.18	0.66	0.0001**
Residual malignant or recurrent lesions (n = 13)	Cirrhotic parenchyma in all patients (n = 50)	ADC ratio	P value
0.91 ± 0.09	1.18 ± 0.07	0.77	0.0001**
Residual malignant or recurrent lesions (n = 13)	Post-treatment parenchymal changes (n = 30)	ADC ratio	P value
0.91 ± 0.09	1.29 ± 0.12	0.70	0.0001**
Entire ablation zone post RF (n = 35)	Entire ablation zone post-MW (n = 15)	P value	
1.38 ± 0.19	1.30 ± 0.16	0.16	
Entire ablation zones in the benign group (n = 37)	Entire ablation zones in the malignant group (n = 13)	P value	
1.37 ± 0.20	1.39 ± 0.09	0.7	

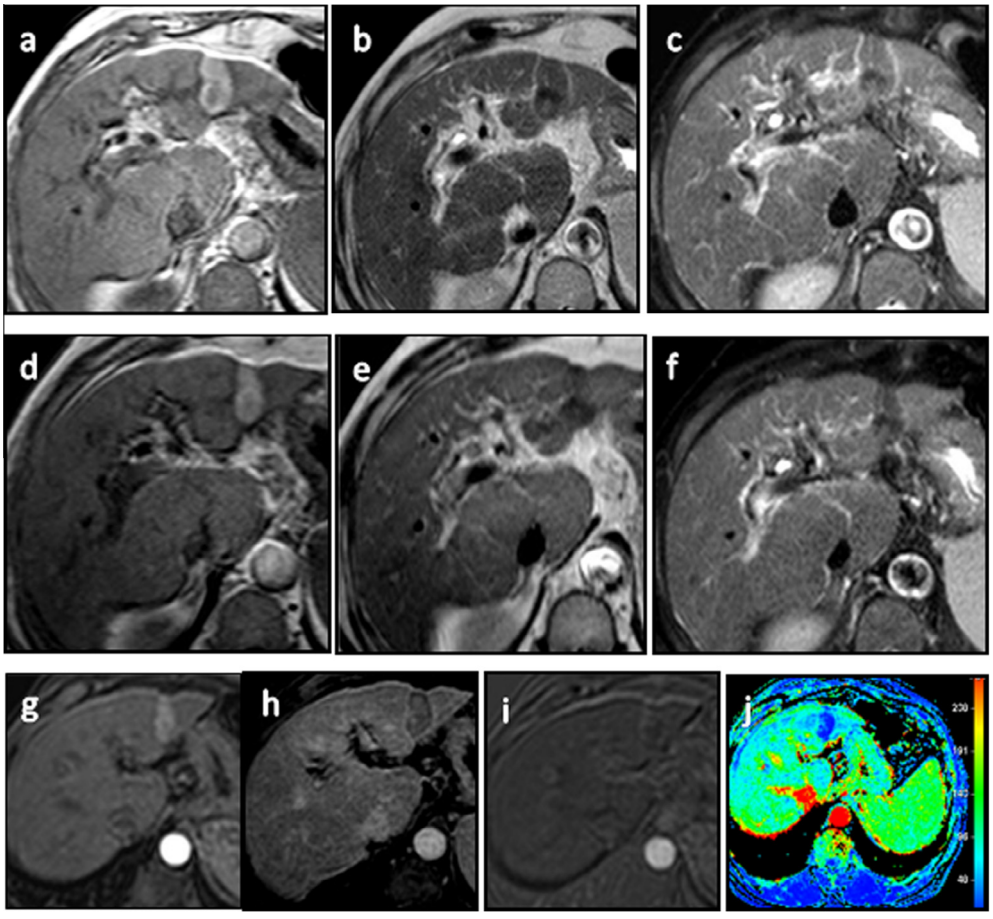

Fig. 3 (a–c) Axial T1, T2 and SPAIR obtained 1 month after microwave ablation of left hepatic lobe HCC in a 54 years old male patient. The ablation zone in the left hepatic lobe elicits high T1 and low T2 and SPAIR signal with peripheral thin rim of low T1 and high T2 signal. (d–f) Axial T1, T2 and SPAIR obtained 4 months after the 1st MRI show that the ablation zone had regressed in size and became of more homogenous signal. (g) Axial arterial phase and (h) axial delayed phase images. The ablation zone appears of high signal in the arterial phase and low signal in the delayed phase, however this is not due to arterial enhancement and delayed washout, but this is due to drop of the signal of the non-enhancing ablation zone relative to the progressively enhancing liver parenchyma. This is proved by the subtracted arterial phase image (i) and the color map image (j) where the lesion appears blue (in the lowest part of the color scale).

the mean ADC of the recurrent or residual malignant lesions (p value 0.0001). There was no statistical difference in the mean ADC values between the entire ablation zones of the resolved and unresolved groups (p value 0.70) and between the entire ablation zone of the microwave and radiofrequency treated lesions (p value 0.16).

4. Discussion

Our study was performed to assess the role of dynamic contrast enhanced and diffusion MR imaging in the assessment of treatment response and detection of tumor viability after

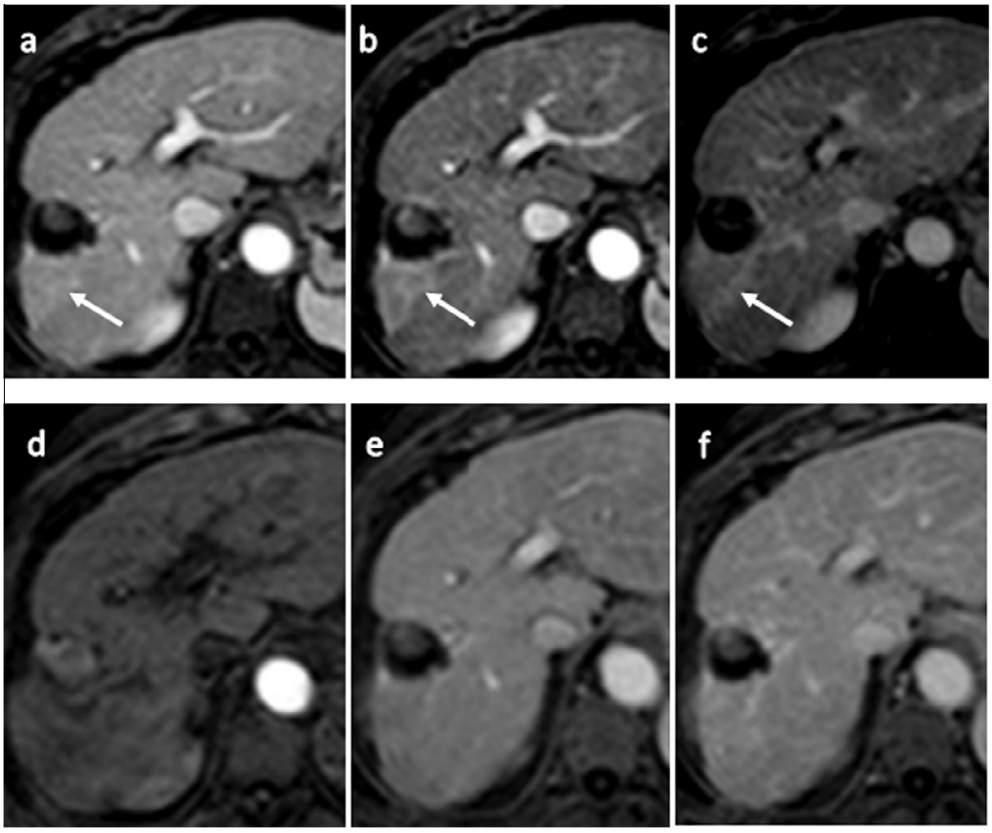

Fig. 4 Axial T1 dynamic study obtained one month (a–c) and 9 months (d–f) after radiofrequency ablation of right lobe hepatocellular carcinoma in 63 year old male. No enhancement noted within the ablation zone or at its margins. The surrounding persistent parenchymal enhancement in the early follow-up MRI (white arrows) almost totally disappeared in the late follow-up study.

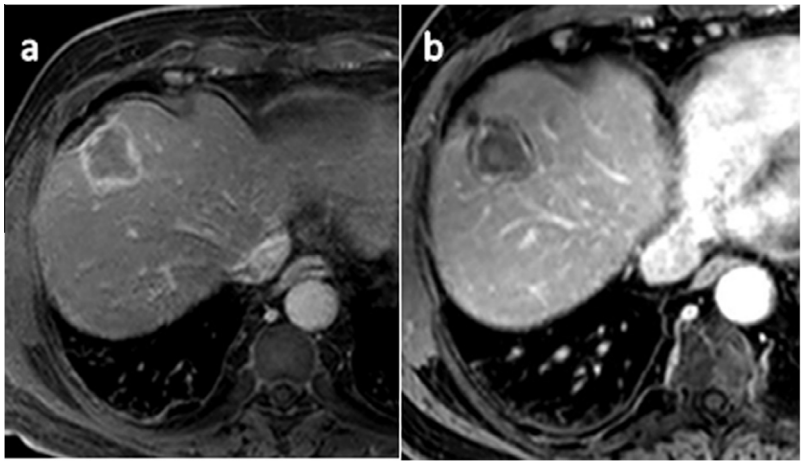

Fig. 5 Axial delayed phase image obtained 5 min after contrast administration (a) one month after ablation and (b) 6 months after ablation of segment VIII hepatocellular carcinoma in 56 years old male patient. Note the regression in the thickness of the enhancing peripheral rim.

radiofrequency and microwave ablation therapy of hepatocellular carcinoma.

The heterogenous signal of the ablation zone in the non-enhanced T1 and in the T2 images in the early post-ablation imaging could be explained by the different tissue changes after ablation including edema, hemorrhage and inflammatory reaction. Such changes are mostly resolved within 4–6 months after ablation leaving only the coagulation necrosis with the characteristic homogenous high T1 and low T2 signal (Fig. 3). Kierans et al. (3) performed a study over 203 ablated lesions for which MRI was acquired after radiofrequency ablation, cryoablation, and microwave ablation. They found that 87.8% of the RF ablation zones imaged within the first 4 months after ablation show high T1 signal with persistence of the high signal in about 84.1% in patients imaged >9 months after ablation.

The absence of significant difference in the signal intensity of the entire ablation zone between the resolved and unresolved groups at the early imaging follow-up could be explained by the fact that the recurrence is mostly at the margin of the ablation zone. This also may be contributed to the post-treatment reactive changes that occur within the ablation zone which may mask any recurrent lesions within the center of the ablation zone (5).

T2 is superior to T1 in detection of recurrent lesions; this could be explained by the higher contrast between the low signal ablation zone and the high signal of the lesion. However at early post-ablation follow-up, the heterogenous T2 signal may mask tumor recurrence, so we cannot depend on T2 signal alone in the early follow-up imaging and correlation with the dynamic study findings is essential in the assessment of the treatment response.

The ill defined perilesional enhancement is found to be a benign finding based on the follow-up study that represents reactive inflammatory and vascular changes of the liver parenchyma adjacent to the ablation zone and this should regress and disappear over time (Fig. 4). With residual or recurrence of the tumor, the area of contrast enhancement is irregular, nodular and thicker and shows contrast washout in the delayed phase (7).

A thin rim surrounding the necrotic cavity can be seen. This rim has low signal intensity on T1, and high signal intensity on T2 images with persistent or delayed post-contrast enhancement and mild diffusion hyperintensity. The histologic analysis

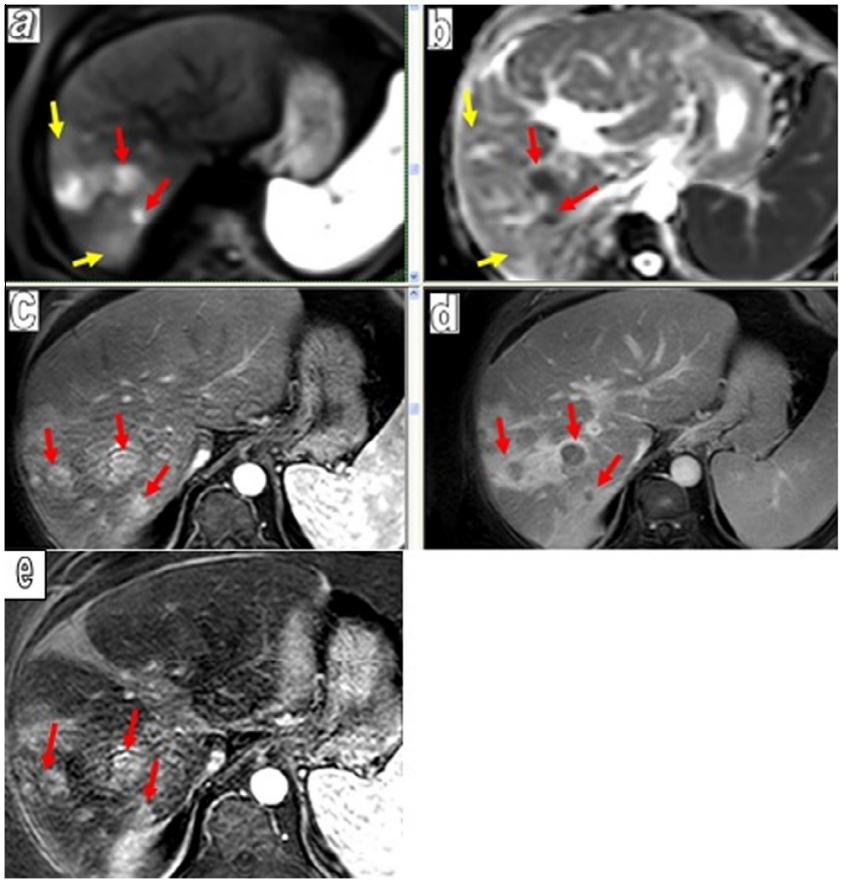

Fig. 6 (a and b) Axial diffusion weighted images (*b* 1000) and corresponding ADC map. (c and d) Axial arterial and delayed phases of the dynamic study and (e) subtracted arterial phase image obtained 3 months after radiofrequency ablation of HCC in a 59 year old male patient. There are multiple nodules (red arrows) and those show arterial enhancement and delayed washout. Note the marked diffusion restriction and low ADC values denoting recurrent HCC in contrast to the surrounding ill defined parenchymal enhancement that shows mild diffusion hyperintensity (yellow arrows) with no corresponding areas of low ADC values. Unfortunately the arterial phase of the dynamic study is partially degraded by respiratory motion artifact however, the diffusion images proved the recurrence of neoplastic lesions.

of the perilesional rim reveals a vascularized inflammatory reaction, hemorrhage, and granulation tissue (8). This peripheral rim most often measures 1–2 mm, but can measure up to 5 mm, and regresses progressively (Fig. 5).

Liquefactive necrosis partly or completely consists of fluid remnants of tissue that became necrotic and was digested by enzymes. Because of the fluid content, liquefactive necrosis appears hyperintense on T2 images (9).

4.1. Role of subtraction technique

The detection of enhancement within the ablation zone is challenging because of the precontrast high T1 signal of the coagulation necrosis. In the early arterial phase the liver parenchyma is mildly enhancing; thus, the ablation zone may preserve its high T1 signal relative to the liver while in the subsequent phases there's progressive parenchymal enhancement, so the non-enhancing ablation zone becomes hypointense relative to the liver that could be misinterpreted as pathologic arterial enhancement and subsequent washout. To solve this problem, dynamic subtraction technique is performed whereby corresponding contrast-enhanced and unenhanced T1-weighted sequences are digitally subtracted image-by-image using the MRI software. The objective of this process is to remove pre-existing T1-weighted high signal from the post-processed images so that the remaining high signal is solely due to enhancement (Figs. 2 and 3). Subtraction MRI improves reader confidence in detecting enhancement in ablation zone and thus improves the overall MRI assessment of the treatment response following locoregional therapy (10). It is essential that the patient's position remains unchanged within the magnet during the unenhanced and contrast enhanced sequences. The patient should be able to maintain a breath-hold throughout the acquisition, and the breath-hold should be reproducible from sequence to sequence. Not fulfilling one or more of these criteria will result in misregistration artifact and image degradation on the subtraction series (11). Several solutions are described to overcome this artifact including imaging at end expiration, image by image subtraction by choosing the images that will be subtracted manually instead of subtracting the whole series and post-processing software

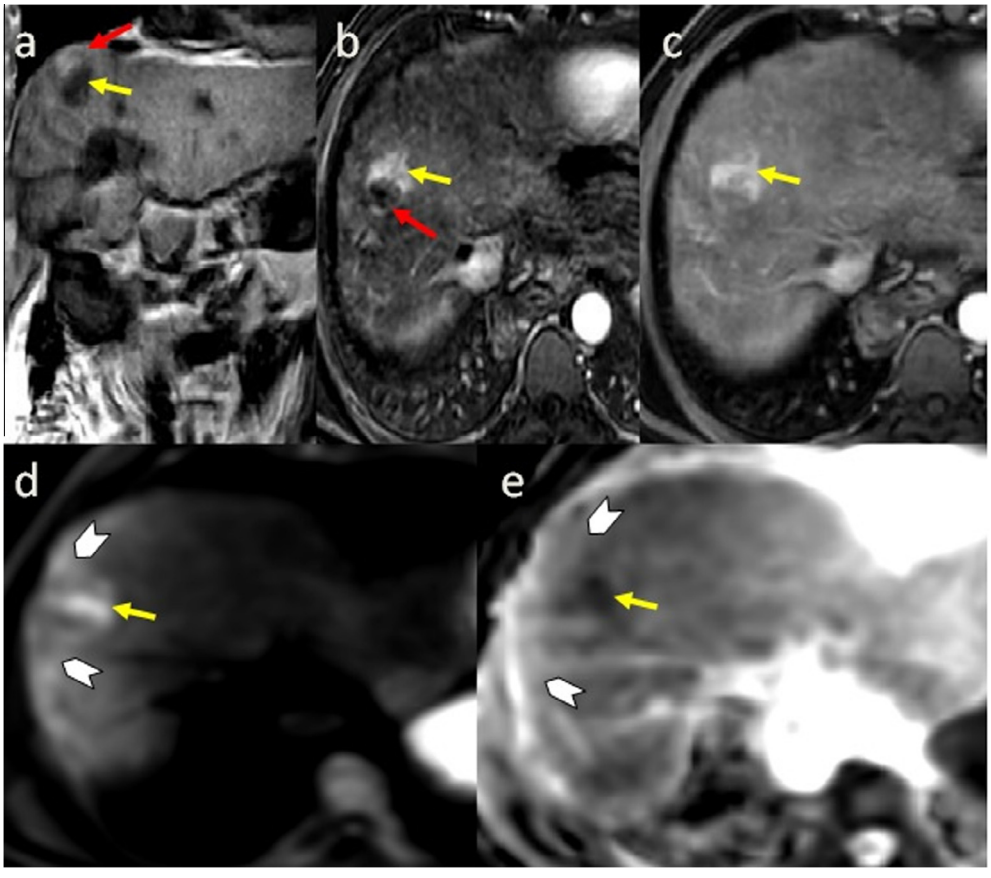

Fig. 7 54 year old male patient after MWA of hepatic focal lesion at segment VIII (a) Coronal T1 weighted images shows the ablation zone (red arrow) eliciting high T1 signal. A large nodule is seen along the anteroinferior margin of the ablation zone elicting low T1 signal (yellow arrow). (b) Subtracted arterial phase image and (c) axial arterial phase image without subtraction show avid enhancement of the nodule without enhancement of the ablation zone (denoting recurrent HCC). (d) Diffusion weighted images (*b* value 800) and (e) ADC map at the same level show restricted diffusion of the malignant nodule (yellow arrows). Note the surrounding parenchymal changes (arrow heads) that appear of high signal in the diffusion images with no signal drop in the corresponding ADC map denoting low cellularity of the benign changes.

algorithms have been developed to improve image matching by performing registration correction on the source data (10).

Precise and accurate arterial phase timing is critical to hepatic lesion detection and characterization. The optimal time to capture arterially enhancing lesions of the liver is slightly later than the time at which the aorta and hepatic artery enhancement peaks (12). The use of multi arterial phase imaging rather than fixed time delay is recommended to ensure that at least one of the phases will capture the lesion at its time of maximum enhancement.

The diffusion analysis revealed significant statistical difference between the therapeutically induced non-tumoral tissue changes (edema, inflammation, fibrosis and necrosis) and the malignant lesions and we detect a cutoff value of 1.05×10^{-3} mm^2/s. This is explained by the fact that benign tissue changes usually show low cellularity and therefore present with less signal in DWI and high ADC value, and can thereby be distinguished from tumoral tissue that presents with high signal in DWI and low ADC value (Figs. 6 and 7) (5).

To our knowledge, the largest study on the role of the diffusion imaging post-radiofrequency ablation was done by Schraml et al. (5) who studied 148 follow-up MR examinations of 54 patients after RFA of malignant focal lesions. They detected mean ADC values of the entire ablation $1.19 \pm 0.30 \times 10^{-3}$ mm^2/s while for the liver parenchyma it was $1.06 \pm 0.21 \times 10^{-3}$ mm^2/s (P value 0.0003). They found that ADC values obtained from the entire ablation zones did not significantly differ between the resolved group ($1.22 \pm 0.30 \times 10^{-3}$ mm^2/s) and the unresolved groups ($1.19 \pm 0.30 \times 10^{-3}$ mm^2/s). They also found that the mean ADC value of the recurrent lesions differs significantly from the mean ADC value of the surrounding parenchymal tissue changes (P value 0.0124). Their results agreed with our results.

4.2. Limitations

Limitations of this study include various time intervals between interventions and follow-up studies, which were determined by clinical practice and not the study design. A further limitation is the lack of histologic proof in most cases, but this is also related to clinical practice where histology is not always indicated.

The measurement of the ADC of the entire ablation zone is not accurate in detection of the recurrent lesion within the center of the ablation zone as it could be masked by the post-ablation changes, however the fact that most of the recurrence occur at the periphery of the ablation zone rather that within its center should be considered. Another limitation in diffusion analysis includes the absence of pre-interventional MRI in most cases so we didn't have the ADC before the treatment.

5. Conclusion

MRI is a powerful tool in the assessment of treatment response and detection of tumor viability after RFA and MWA of hepatocellular carcinoma. Radiologists should be familiar with the imaging appearance of the normal ablation zones and benign post-ablation changes in order to detect malignant lesions. Imaging protocol should include dynamic study combined with diffusion imaging with post-processing of the images to obtain subtracted images and color mapping for better tissue characterization and should be performed at regular time intervals. Dynamic study is the cornerstone in detection of recurrent lesions while ADC measurements can differentiate between malignant lesions and post-treatment benign parenchymal changes. Well defined nodular enhancement, thick irregular marginal enhancement or gross enlargement of the lesion with arterial phase enhancement and contrast washout were considered positive for malignancy, while ill-defined persistent enhancement or well defined rim marginal enhancement is considered as benign post-ablation changes.

Conflict of interest

The authors declare that there are no conflict of interests.

References

(1) Özkavukcu E, Haliloğlu N, Erden A. Post-treatment MRI findings of hepatocellular carcinoma. Diagn Interv Radiol 2009;15:111–20.
(2) Smith S, Gillams A. Imaging appearances following thermal ablation. Clin Radiol 2008;63:1–11.
(3) Kierans S, Elazzazi M, Braga L, et al. Thermoablative treatments for malignant liver lesions: 10-year experience of MRI appearances of treatment response. AJR 2010;194:523–9.
(4) Kim KW, Lee JM, Choi BI. Assessment of the treatment response of HCC. Abdom Imaging 2011;36:300–14.
(5) Schraml C, Schwenzer N, Clasen S, et al. Navigator respiratory-triggered diffusion-weighted imaging in the follow-up after hepatic radiofrequency ablation—initial results. J Magn Reson Imaging 2009;29:1308–16.
(6) Chopra S, Dodd III GD, Chintapalli KN, et al. Tumor recurrence after radiofrequency thermal ablation of hepatic tumors: spectrum of findings on dual-phase contrast-enhanced CT. AJR 2001;177:381–7.
(7) Clasen S, Boss A, Schmidt D, et al. Magnetic resonance imaging for hepatic radiofrequency ablation. Eur J Radiol 2006;59:140–8.
(8) Goldberg SN, Gazelle GS, Compton CC, et al. Treatment of intrahepatic malignancy with radiofrequency ablation: radiologic–pathologic correlation. Cancer 2000;88:2452–63.
(9) Braga L, Guller U, Semelka RC. Pre-, peri-, and post-treatment imaging of liver lesions. Radiol Clin North Am 2005;43:915–27.
(10) Winters SD, Jackson S, Armstrong GA, et al. Value of subtraction MRI in assessing treatment response following image-guided loco-regional therapies for hepatocellular carcinoma. Clin Radiol 2012;67:649–55.
(11) Newatia A, Khatri G, Friedman B, et al. Subtraction imaging: applications for nonvascular abdominal MRI. AJR 2007;188:1018–25.
(12) Sharma P, Kitajima HD, Kalb B, et al. Gadolinium enhanced imaging of liver tumors and manifestations of hepatitis: pharmacodynamic and technical considerations. Top Magn Reson Imaging 2009;20(2):71–80.